STEM CELLS

TISSUE-SPECIFIC STEM CELLS

Persistent Wnt/β-Catenin Signaling Determines Dorsalization of the Postnatal Subventricular Zone and Neural Stem Cell Specification into Oligodendrocytes and Glutamatergic Neurons

KASUM AZIM,[a] BRUNO FISCHER,[a] ANAHI HURTADO–CHONG,[a] KALINA DRAGANOVA,[b] CLAUDIO CANTÙ,[c] MARTINA ZEMKE,[b] LUKAS SOMMER,[b] ARTHUR BUTT,[d] OLIVIER RAINETEAU[a,e,f]

Key Words. Cell signaling • Stem cell plasticity • Progenitor cells • Oligodendrocytes • Neural stem cell • Nervous system • Neural induction • Neuron

ABSTRACT

In the postnatal and adult central nervous system (CNS), the subventricular zone (SVZ) of the forebrain is the main source of neural stem cells (NSCs) that generate olfactory neurons and oligodendrocytes (OLs), the myelinating cells of the CNS. Here, we provide evidence of a primary role for canonical Wnt/β-catenin signaling in regulating NSC fate along neuronal and oligodendroglial lineages in the postnatal SVZ. Our findings demonstrate that glutamatergic neuronal precursors (NPs) and oligodendrocyte precursors (OPs) are derived strictly from the dorsal SVZ (dSVZ) microdomain under the control of Wnt/β-catenin, whereas GABAergic NPs are derived mainly from the lateral SVZ (lSVZ) microdomain independent of Wnt/β-catenin. Transcript analysis of microdissected SVZ microdomains revealed that canonical Wnt/β-catenin signaling was more pronounced in the dSVZ microdomain. This was confirmed using the β-catenin-activated Wnt-reporter mouse and by pharmacological stimulation of Wnt/β-catenin by infusion of the specific glycogen synthase kinase 3β inhibitor, AR-A014418, which profoundly increased the generation of cycling cells. *In vivo* genetic/pharmacological stimulation or inhibition of Wnt/β-catenin, respectively, increased and decreased the differentiation of dSVZ-NSCs into glutamatergic NPs, and had a converse effect on GABAergic NPs. Activation of Wnt/β-catenin dramatically stimulated the generation of OPs, but its inhibition had no effect, indicating other factors act in concert with Wnt/β-catenin to fine tune oligodendrogliogenesis in the postnatal dSVZ. These results demonstrate a role for Wnt/β-catenin signaling within the dorsal microdomain of the postnatal SVZ, in regulating the genesis of glutamatergic neurons and OLs. STEM CELLS *2014;32:1301–1312*

[a]Brain Research Institute, University of Zürich/ETHZ, Zürich, Switzerland; [b]Institute of Anatomy, University of Zürich, Zürich, Switzerland; [c]Institute of Molecular Life Sciences, University of Zürich, Zürich, Switzerland; [d]Institute of Biomedical and Biomolecular Sciences, School of Pharmacy and Biomedical Sciences, Portsmouth University, Portsmouth, United Kingdom; [e]Stem Cell and Brain Research Institute, INSERM U846, Lyon, France; [f]Universite de Lyon, Universite Lyon I, 69003 Lyon, France

Correspondence: Arthur Butt, PhD, Institute of Biomedical and Biomolecular Sciences, School of Pharmacy and Biomedical Sciences, Portsmouth University, Portsmouth, U.K. Telephone: +44 23 9284 2156; Fax: +44 23 9284 3082; e-mail: arthur.butt@port.ac.uk; or Olivier Raineteau, PhD, Brain Research Institute, University of Zürich/ETHZ, Zürich, Switzerland. Telephone: +41 44 635 32 88; Fax: +41 44 635 3303; e-mail: raineteau@hifo.uzh.ch

Received July 29, 2013; accepted for publication December 6, 2013; first published online in STEM CELLS *EXPRESS* January 21, 2014.

1066-5099/2014/$30.00/0

http://dx.doi.org/10.1002/stem.1639

INTRODUCTION

In the central nervous system (CNS), neuronal generation in the postnatal and adult brain is restricted to highly localized germinal niches, most notably the subventricular zone (SVZ) located in the forebrain lateral ventricle (LV). Neural stem cells (NSCs) of the postnatal and adult SVZ primarily give rise to olfactory neurons and oligodendrocytes (OLs), the myelinating cells of the CNS [1–3]. SVZ-NSCs (also referred as type-B cells) give rise to actively proliferating transiently amplifying cells, named type-C cells that either differentiate into neuronal precursors (NPs, type-A cells) or oligodendrocyte precursor cells (OPs) [4]. NPs migrate along the rostral migratory stream to the olfactory bulb, where they differentiate into phenotypically distinct populations of interneurons [2, 5], while OPs migrate throughout the forebrain to differentiate into myelinating OLs [6]. Recent studies indicate that the neurogenic fate of SVZ-NSCs depends on their location within microdomains of the SVZ [7–11], whereby NSCs in the dorsal SVZ (dSVZ) give rise to OPs and glutamatergic neurons of the olfactory bulb [6, 12, 13], and NSCs located in both the dorsal and lateral SVZ (lSVZ) generate distinct subtypes of GABAergic interneurons [5, 14]. Moreover, transcription factors that are involved in the early specification of SVZ-NSCs toward the different lineages are expressed in defined SVZ microdomains [9, 12, 14]. For example, the NP transcription factor Tbr2 (also referred to as Eomes) that regulates differentiation of glutamatergic neurons is largely restricted to the dSVZ, together with the OL lineage transcription factor Olig2 [13, 15]. In contrast, the NP transcription factor Dlx2 that regulates the differentiation of GABAergic neurons is enriched in

the lSVZ [14]. Although it was thought that heterogeneity of SVZ-NSC fates is intrinsically coded, a recent study identified Shh as a ventralizing factor in the adult SVZ, where Shh was able to respecify dSVZ-NSCs to acquire ventral neuronal fates [16]. In contrast, the factors that maintain SVZ-NSC dorsalization postnatally are unresolved, but canonical Wnt/β-catenin signaling has been identified as an important dorsalizing factor during embryonic (E9.5) cortical development [17]. Furthermore, a role for Wnt/β-catenin has been described in the adult SVZ, where it controls proliferation of NSCs and NPs [18], although another study suggested Wnt signaling has opposing roles in the developing and the adult brain, being more important in NSC differentiation in the latter, rather than proliferation [19]. Similarly, studies in which Wnt/β-catenin signaling was constitutively activated in OL lineage cells indicated that this signaling pathway regulates postnatal OL differentiation, but not proliferation [20]. In contrast, we found that stimulation of Wnt/β-catenin signaling with the Wnt mimetic AR-A014418 increased both proliferation and differentiation of OL lineage cells *in vivo* in the postnatal forebrain [21]. This is consistent with a recent study in the adult indicating a specific role for canonical Wnt signaling in selectively stimulating proliferation within the OL lineage, without changing lineage choice or proliferation within neurogenic clones [22].

Hence, there is increasing evidence that Wnt/β-catenin signaling in the SVZ persists after birth, but its potential role in regulating fate specification of NSCs within SVZ microdomains has not been investigated so far. Here, we show that canonical Wnt/β-catenin signaling is primarily active in the dSVZ of the postnatal forebrain and selectively regulates the fate of dSVZ-NSCs into OPs and glutamatergic NPs.

Materials and Methods

Unless otherwise stated, materials were obtained from Sigma-Aldrich (Buchs, Switzerland, www.sigmaaldrich.com). All experiments on animals were performed in agreement with the Canton of Zurich veterinary office guidelines. All transgenic mice were maintained in a BL/6 background. For *in vivo* experiments, pups were anesthetized by hypothermia.

SVZ Microdissection

SVZ microdomains were microdissected using previously published protocols [15]. In brief, mice aged postnatal day 6 (P6) were killed humanely by cervical dislocation and brains were rapidly dissected and placed in ice-cold postnatal-specific coronal brain matrix (Zivic Instruments, Pittsburgh, PA, www.zivicinstruments.com). Tissue segments of 500 μm thickness containing the rostral LV were isolated and the lSVZ and dSVZ were microdissected for subsequent analysis by real-time quantitative polymerase chain reaction (rt-qPCR) or Western blot. One litter was used to pool sufficient quantities of microdissected tissue for subsequent Western blot or RNA extraction for 1 "*n*" value.

RNA Extraction, Amplification, and rt-qPCR

Maintaining strict RNase-free and sterile conditions throughout, RNA was amplified using 3 ng as input material for all samples with the Nugene Pico Oviation WT kit (NuGEN Technologies, Inc., San Carlos, CA, www.nugeninc.com) following manufacturer's guidelines. Synthesized cDNA was purified using Qiagen MinElute reaction clean up kit (Qiagen, Valencia, CA, www.qiagen.com). For rt-qPCR, amplified cDNA was loaded with 5 μM of forward and reverse primers, SYBR green mastermix, and DNAase/RNase-free H_2O onto 96-well plates for Lightcycler 480 (Roche Diagnostics, Rotkreuz, Switzerland, www.roche-diagnostics.com). Relative gene expression was determined using the $^{\Delta\Delta}-$ct method *versus* the housekeeping gene glyceraldehyde-3-phosphate dehydrogenase (GAPDH). See Supporting Information Table S1 for list of primers and their source. Gene expression data are presented as mean $\pm$ standard error of the mean (SEM), and samples compared for significance using unpaired *t* test (*t* test) in Prism v3.02 software; (GraphPad, La Jolla, CA, www.graphpad.com).

Pharmacological Stimulation of Wnt/β-Catenin

As previously described, the Wnt/β-catenin pathway was activated pharmacologically by intraventricular infusion of the glycogen synthase kinase 3β (GSK3β) inhibitor AR-A014418 into the LV to achieve a concentration of 6 μM/l in the ventricular cerebrospinal fluid (CSF), which we have shown effectively inhibits GSK3β in periventricular regions, as determined by phosphorylation of Ser9-GSK3β [21]. Sterile saline/DMSO vehicle was used as a control.

Western Blot

AR-A014418 was infused into the LV of both hemispheres at P6, and animals were sacrificed 45 minutes after the final AR-A014418 infusion. Microdissected SVZ microdomains were snap frozen, briefly centrifuged at 4,000*g* to obtain tissue pellets, and protein extracted with ice-cold lysis buffer containing protease inhibitors. Lysed tissue supernatant was transferred to Ultrafree MC centrifugal spin columns (Millipore, Zug, Switzerland, www.millipore.com) for separation and concentration of protein extracts above 15 kDa. Cytoplasmic and nuclear extracts were obtained using the "NE-PER Nuclear and Cytoplasmic Extraction" kit (Thermo Fisher Scientific, Waltham, MA, www.thermofisher.com) and protein concentration determined by Bradford protein assay. Standard procedures were followed. See Supporting Information Table S2 for a list of primary antibodies and species-matched secondary HRP-conjugated secondary antibodies, all used at 1:1,000 (Dako; Baar, Switzerland, www.dako.com). Protein bands were detected by adding SuperSignal West Pico Chemiluminescent Substrate (Pierce, Waltham, MA, www.thermofisher.com) and by exposing the blot in a Stella detector (Raytest, Straubenhardt, Germany, www.raytest.com). Densitometry analysis was performed with NIH software by normalizing the band intensities to total GSK3β or, in the case of β-catenin, to β-actin or Lamin B1.

Transgenic Mouse Lines

For analysis of canonical Wnt/β-catenin signaling, we used the β-catenin-activated transgene reporter transgenic mouse line (also referred to as Bat-Gal mice), in which the *lacZ* gene is under the control of seven consensus Lef1/Tcf-binding motifs driving the expression of the β-Galactosidase reporter, termed "βGal" [23]. For gain-of-function experiments, the β-catenin^{exon3} mouse line was used. Exon3 of β-catenin

contains a phosphorylation site that targets β-catenin to degradation; and in this mouse line, the floxed exon3 is removed upon Cre-mediated recombination, resulting in a constitutive stabilized form of β-catenin [24]. For loss-of-function experiments, the β-catenin floxed mouse line (β-catenin$^{lox/lox}$) was used (Jax mouse stock: 004152, Bar Harbor, ME, www.jaxmice.jax.org), in which loxP sites are inserted in intron 1 and intron 6, so that recombination induces deletion of exons 2–6, resulting in ablation of β-catenin [25]. In addition, we used the signaling mutant line β-catenin$^{dm/lox}$, in which endogenous β-catenin protein is replaced by a mutant form that maintains the cell adhesion functions of β-catenin, but upon Cre-mediated recombination, its Lef1/Tcf-binding domains are removed, thus preventing the activation of canonical Wnt/β-catenin nuclear targets [26]. Mice were genotyped as previous [26].

Plasmid Preparation and Postnatal Electroporation

A pCAGs-Cre:GFP plasmid and control plasmid pCAGs-green fluorescent protein (GFP) under a chicken β-actin promoter were obtained from Addgene (Cambridge, MA, www.addgene.org, plasmids 13775; 11150). Control plasmid lacked the Cre-recombinase coding sequence (pCAGs-GFP). Plasmids were amplified and purified using the Qiagen EndoFree Plasmid Maxi Kit following manufacturer's guidelines (Qiagen, Valencia, CA, www.qiagen.com). The βGal plasmid used to identify active Wnt signaling in transfected cells codes for a nuclear β-Galactosidase reporter, was obtained from Addgene (20889) and is the same construct as the Bat-Gal reporter mouse strain described above [23]. Electroporation of NSCs in direct contact with the ventricular surface was performed as previously described [8]. Mice aged P2 were electroporated and analyzed 4 days later. In the case of pharmacological stimulation of Wnt/β-catenin, CD1 mice were electroporated at P3 and were then infused with AR-A014418 at P4 and P5, prior to analysis at P6.

Enhancement or ablation of β-catenin transcriptional activity in the β-catenin^{exon3} and β-catenin$^{lox/lox}$ mice (see above) was confirmed by coelectroporating the βGal reporter plasmid with the GFP:Cre fusion plasmid [23]. Cre-mediated recombination successfully enhanced or reduced transfected cells βGal nuclear expression in the β-catenin^{exon3} or β-catenin$^{lox/lox}$ mice, respectively (Supporting Information Fig. S1), validating our targeted-electroporation approach to manipulate Wnt/βcatenin signaling.

Immunohistochemistry

Pups were injected intraperitoneally with an overdose of pentobarbital (Eutha77 in Ringer's solution), followed by transcardial perfusion of 2.5 ml Ringer's solution and 5 ml 4% paraformaldehyde (PFA) dissolved in phosphate buffered saline (pH 7.4). Brains were dissected and postfixed in PFA for 48 hours at 4°C, then processed for immunohistochemistry, as previously described [9]. Primary antibodies from different species were used, as stated in Supporting Information Table S2, followed by species-matched alexa-488, -555, or -647-conjugated secondary antibodies (Life Technologies, Zug, Switzerland, www.lifetechnologies.com), or biotinylated antibodies (Jackson Immunoresearch, Suffolk, United Kingdom, www.jir-europe.com) followed by alexa-conjugated Streptavidin for 30 minutes. EdU was given subcutaneously 3 hours before sacrifice to detect cells in active S-phase and previous protocols followed to visualize nucleotide incorporation [9]. Sections were counterstained with DAPI and/or Topro3 (Invitrogen) and coverslipped with antifading mounting medium (Vectashield, Vector Labs, Peterborough, United Kingdom, www.vectorlabs.com) or ProlongGold (Life Technologies, Zug, Switzerland, www.lifetechnologies.com).

Imaging and Quantification Procedures

Imaging and analysis methods are described in detail in our previous methodological study [8]. Electroporation efficiencies vary per animal by ∼20%, therefore differences in marker expression (Tbr2/Dlx2/Olig2) are indicated as the change in ratios/fate-switch per total number of GFP-expressing cells per series throughout the rostro-caudal axis per animal. For glial fibrillary acidic protein (GFAP)/Mash1/Dcx quantifications, the same procedures were followed by selecting constant fields of view between experimental groups within ∼70 μm from the boundary of the ventricular surface as described previously [9]. Colocalization was assessed by confocal 3D reconstruction on a Leica SPE II (Leica, Wetzlar, Germany, www.leica.com) or an Olympus FluoView FV1000 (Olympus, Volketswil, Switzerland, www.olympus.ch) confocal microscope equipped with a ×40 objective (N.A. 1.25). For densitometric quantification procedures, ∼70 μm from the ventricular surface in 30 μm stacks with 2 μm intervals of each entire SVZ microdomain was analyzed using standard procedures in ImageJ (National Institute of Health, Bethesda, MD, www.imagej.nih.gov). At least three individual animals, each representing 1 *n* value, were analyzed for all βGal quantifications. At least five individual animals, each representing 1 *n* value, were analyzed in all electroporation experiments. For all electroporation experiments, an average of 446.2 transfected cells/animal in serial sections encompassing the entire rostral-caudal axis of the LV was analyzed. At least four individual animals, each representing 1 *n* value, were analyzed in all pharmacological gain-of-function experiments. Analyses are presented as mean ± SEM, and samples were compared for significance using unpaired *t* test (*t* test) or ANOVA followed by Bonferroni's post hoc test (Prism v3.02; GraphPad, La Jolla, CA, www.graphpad.com).

Results

Wnt/β-Catenin Signaling Is Enriched Within the Dorsal SVZ Microdomain

Gene expression profiles were performed on microdissected dSVZ and lSVZ microdomains, normalizing transcript levels against housekeeping genes by the comparative $^{\Delta\Delta}$-ct method (Fig. 1A, 1B), as described previously [15]. The results show that transcripts for the early pallial NSC marker, Emx1, the glutamatergic NP transcription factor, Tbr2, and the OP transcription factors, Olig2 and Sox10, were significantly enriched in the dSVZ, while Tbr2 was essentially absent from the lSVZ (Fig. 1A; $p < .01$; *t* test). By comparison, transcripts for the early subpallial NSC marker Gsx2 and the GABAergic NP transcription factor Dlx2 were highly enriched in the lSVZ, respectively (Fig. 1A; $p < .05$; *t* test). These results confirm that SVZ microdissection provides a reproducible method for analyzing differences

between SVZ microdomains [15], and support evidence that OPs and glutamatergic interneurons of the olfactory bulb are derived from the dSVZ, whereas the lSVZ has the greatest neurogenic potential for GABAergic interneurons. The Wnt-target genes Fzd1, Axin2, and Lef1 were significantly and specifically enriched in the dSVZ (Fig. 1B; $p < .05$, *t* test). Notably, the Shh-target gene Gli1 was enriched in the lSVZ (Fig. 1B; $p < .05$, *t* test), consistent with its role as a ventralizing factor in the adult SVZ [16]. We also analyzed transcripts for canonical Wnt ligands Wnt3, Wnt3a, Wnt5a, Wnt7a, and Wnt8b in the SVZ and in the choroid plexus, a previously described source of Wnt ligands [27, 28]. In the SVZ, we detected expression only for Wnt3 and Wnt7a. Only Wnt3 showed a dorsal enrichment (Fig. 1C, $p < .05$, *t* test) while Wnt7a was homogeneously expressed between the SVZ microdomains (not presented), supporting evidence that Wnt3 is a key factor in the postnatal dSVZ [22]. All tested Wnt transcripts were also detected in the choroid plexus although at different levels (Fig. 1C), consistent with this tissue being a major source of Wnt ligands in the postnatal brain [27, 29]. The results identify the dSVZ as a previously unrecognized niche for Wnt/β-catenin signaling in the postnatal brain.

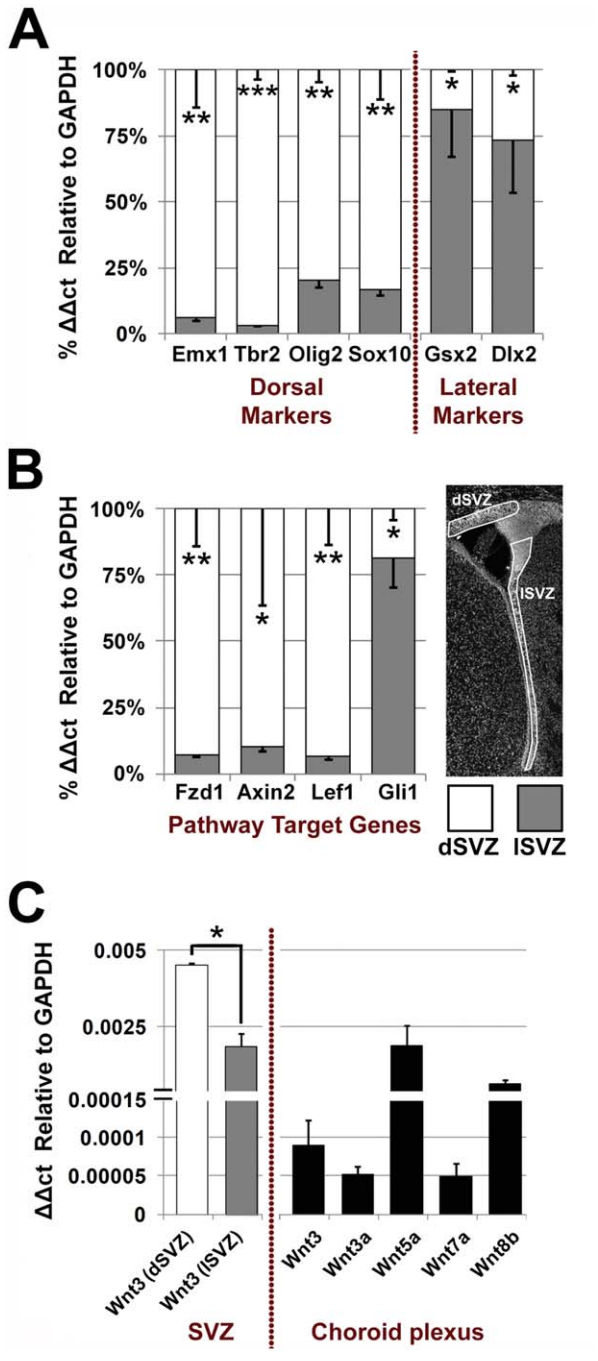

Functional Wnt/β-Catenin Signaling Is Localized to the Dorsal SVZ Microdomain

To identify the regional and cellular localisation of canonical Wnt/β-catenin signaling in SVZ microdomains, we used the Bat-Gal reporter transgenic mouse line [23] and infusion of the Wnt mimetic AR-A014418 [18, 21]. In the Bat-Gal mice, β-Galactosidase (βGal) expression at P6 was greatest dorsally and declined ventrally (Fig. 2A). Throughout the SVZ, βGal+ cells were most dense within the dSVZ, with little expression detected in the lSVZ (Fig. 2B). Immunostaining demonstrated that the majority of βGal+ cells in the dSVZ were GFAP+ NSCs or coexpressed the proliferative marker Ki67, an indication that they were actively proliferating transient amplifying cells (Fig. 2C). βGal+ cells also coexpressed the glutamatergic NP marker Tbr2 and the OP marker Olig2 (Fig. 2D), demonstrating functional Wnt/β-catenin signaling in glutamatergic NPs and OL lineages derived from the dSVZ. Localization of functional Wnt/β-catenin signaling in the SVZ was examined further by infusion of AR-A014418, which inhibits GSK3β to prevent phosphorylation of β-catenin, leading to its nuclear translocation and activation of canonical Wnt/β-catenin targets [18, 21]. Western blot analysis of SVZ microdomains 45 minutes following AR-A014418 infusion demonstrated significant inhibition of GSK3β compared to controls, as determined by phosphorylation of Ser9-GSK3β, and this was significantly greater in the dSVZ compared to the lSVZ (Fig. 2E, 2F; $p < .05$, ANOVA followed by Bonferroni's post hoc test). In agreement, detection of β-catenin in nuclear extracts demonstrated significantly greater Wnt/β-catenin signaling in the

Figure 1. Heterogeneous pallial/subpallial marker expression and Wnt-expression/activities in postnatal SVZ microdomains. **(A):** SVZ microdomains were microdissected as previous to obtain cDNA for real-time quantitative polymerase chain reaction (rt-qPCR) of gene expression at P6 [15]. These revealed significant enrichment of pallial markers (Emx1/Tbr2) and oligodendrocyte lineage markers (Olig2/Sox10) *versus* subpallial markers (Gsx2/Dlx2) (*t* test) in dSVZ *versus* lSVZ, respectively. **(B):** Downstream Wnt-target genes Fzd1, Axin2, and Lef1 are significantly enriched in the dSVZ compared to the lSVZ and conversely Shh-target gene Gli1 is enriched in the lSVZ (*t* test). White and gray bars in (A, B) specify the dSVZ and lSVZ, respectively. The coronal, nuclear counterstained section indicates the location of the microdissected SVZ microdomains. **(C):** The expression levels of canonical Wnt ligands transcripts were assayed by rt-qPCR in the dSVZ (white bar), lSVZ (gray bar), and choroid plexus (black bars). Error bars represent the SEM of ≥ 3 *n* numbers. ***, $p < .001$; **, $p < .01$; *, $p < .05$; *t* test. Abbreviations: GAPDH, glyceraldehyde-3-phosphate dehydrogenase; SVZ, subventricular zone; dSVZ, dorsal SVZ; lSVZ, lateral SVZ.

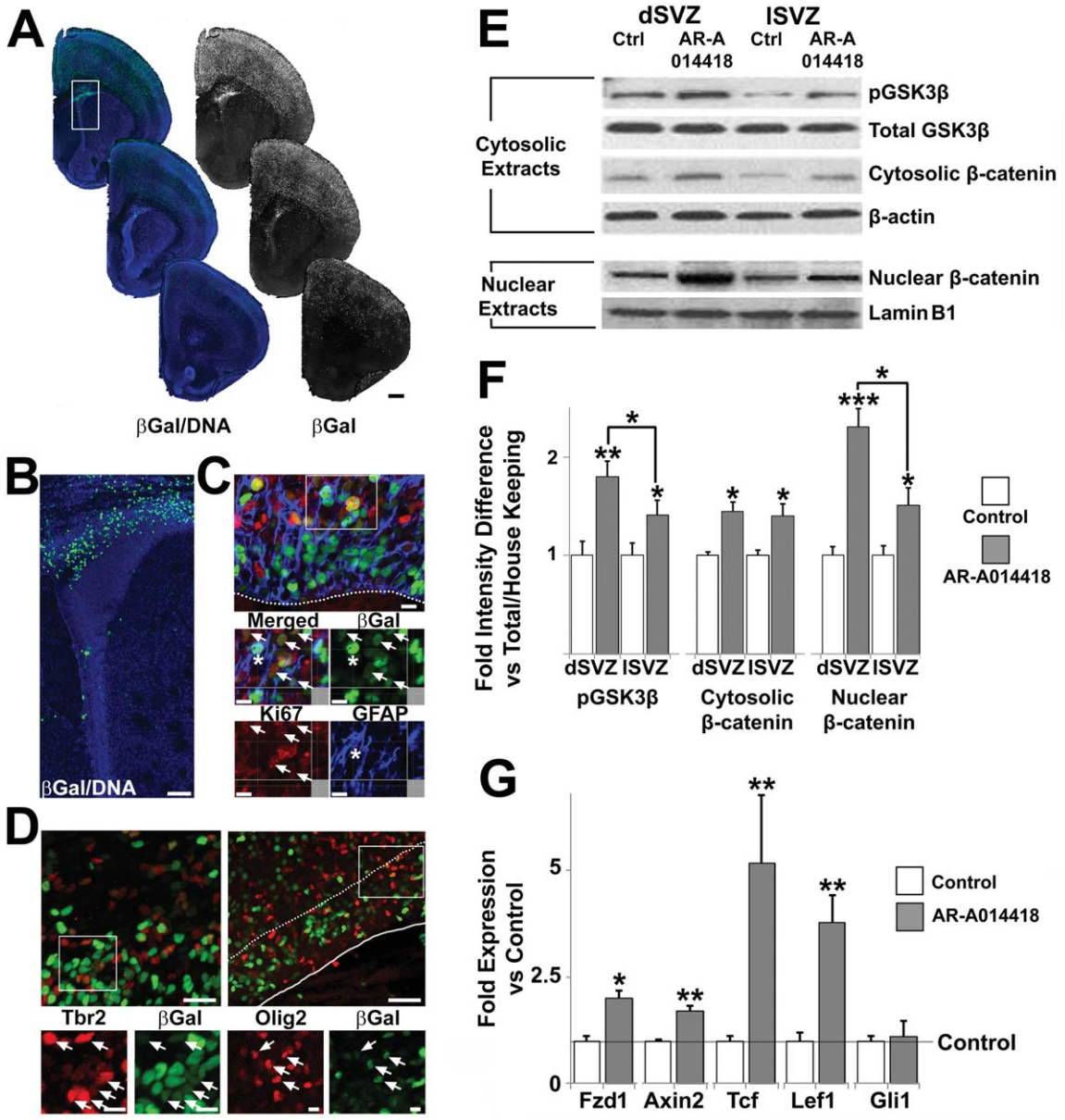

Figure 2. Functional Wnt/β-catenin signaling is localized to the dSVZ microdomain. **(A, B):** Overview of equally spaced rostral forebrain sections of the Bat-Gal Wnt-reporter mouse line at P6 illustrating that expression of βGal (green) is enriched in dSVZ regions and declines ventrally as exemplified in the higher magnification periventricular section in (B) (blue: DNA counterstain). **(C):** GFAP+ and Ki67+ cells readily coexpress βGal (asterisk and arrows, respectively) in the dSVZ regions with greater βGal expression closer to the lateral ventricle wall (dotted line). **(D):** Confocal micrographs illustrate presence of βGal+/Tbr2+ and βGal+/Olig2+ cells in the dSVZ. Captions indicate colocalizing cells (arrows). Scale bars = 500 μm (overview, A); 100 μm (B and overview, D); 10 μm (inserts) in (C) and (D). **(E):** Pups received an intraventricular infusion of AR-A014418 or saline/DMSO as control vehicle and were sacrificed 45 minutes later and SVZ microdissected for Western blot. Inactivity (ser9 state) of pGSK3β, total GSK3β (internal control), β-catenin, and β-actin (loading control) in cytosolic extracts and levels of β-catenin nuclear extracts *versus* Lamin B1 (loading control) were determined. **(F):** Data are mean densitometric percentage change in values and the SEM from $n > 3$ replicates (***, $p < .001$; **, $p < .01$; *, $p < .05$; ANOVA followed by Bonferroni's post hoc test). White bars are the controls and gray bars are the AR-A014418 intensity values. **(G):** AR-A014418 or saline/DMSO was infused intraventricularly and the dSVZ microdissected 2.5 hours later for subsequent real-time quantitative polymerase chain reaction determination of Wnt-target gene transcripts. Changes in transcripts were compared *versus* control as a percentage. Data are expressed as fold change relative to expression values (vs. GAPDH) and the SEM (error bars). White bars are the controls and gray bars are the AR-A014418 intensity values. **, $p < .01$; *, $p < .05$; *t* test. Abbreviations: dSVZ, dorsal subventricular zone; lSVZ, lateral SVZ; βGal, Beta-Galactosidase; GFAP, Glial Fibrillary Acidic Protein; Ctrl, Control; pGSK3β, phospho-GSK3β.

dSVZ than in the lSVZ (Fig. 2E, 2F; $p < .05$, ANOVA followed by Bonferroni's post hoc test). In addition, rt-qPCR demonstrated that transcripts for Wnt/β-catenin targets Fzd1, Axin2, Tcf, and Lef1 were all significantly upregulated in the dSVZ 2.5 hours following infusion of AR-A014418, whereas the Shh-target gene Gli1 was unaltered (Fig. 2G; *t* test, see graph for individual *p* values) (see list and references in www.stanford.edu/group/nusselab/cgi-bin/wnt/target_genes). Examination of

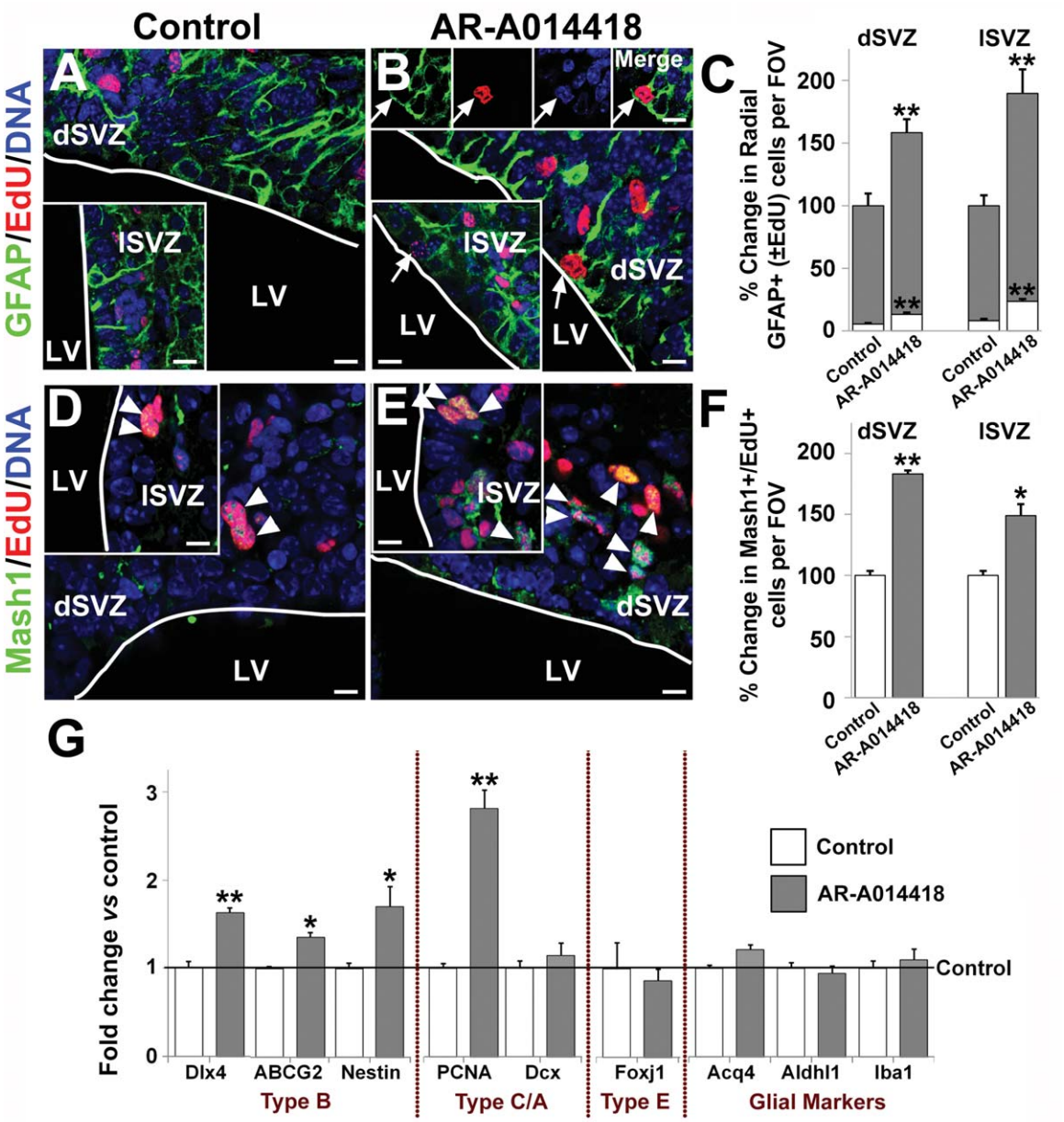

Figure 3. Wnt/β-catenin signaling stimulates type-B and type-C cell proliferation in the lSVZ and dSVZ microdomains. Pups aged P4 were infused with AR-A014418 or saline/DMSO as control vehicle for 2 days and forebrains examined at P6 for immunolabeling of type-B (i.e., GFAP) and type-C (i.e., Mash1) cell markers. EdU was given subcutaneously 3 hours before sacrifice to determine cells in active cell cycle. **(A, B):** Radial-like GFAP+ cells, both proliferative (EdU+) and nonproliferative (EdU−), were present at greater densities following AR-A014418 infusion in either SVZ subregions. Arrows indicate proliferating radial GFAP+ cells in insets of (B). Upper inset of (B) shows cropped single plane and single channel images of colocalizing expression of GFAP and EdU. **(C):** Quantification of nonproliferating radial GFAP+/EdU− (gray bars) and proliferating radial GFAP+/EdU+ (white bars) showed a similar increase in either SVZ subregion following AR-A014418 infusion. Data are mean percentage of cells quantified in each region in a constant volume (fields of view [FOV]) and the SEM (error bars); $n \geq 4$ animals (**, $p < .01$; *t* test). **(D–F):** Actively proliferating progenitors (Mash1+/EdU+) showed a similar increase in either SVZ subregions following AR-A014418 infusion. Arrowheads exemplify double positive cells. Mash1+/EdU− cells were rare. (F): Quantification of Mash1+/EdU+ cells in the SVZ microdomains following saline/DMSO (white bars) or AR-A014418 (gray bars) infusions. Data are mean percentage of cells quantified in each region in a constant volume (FOV) and SEM (error bars); $n \geq 4$ animals. Scale bars = 10 μm. **(G):** AR-A014418 or saline/DMSO was infused and the dSVZ microdissected 2.5 hours following infusion for subsequent rt-qPCR determination of mRNA transcripts enriched in specific SVZ cells types. Changes in transcripts were compared *versus* control as a percentage. Data are expressed as fold change relative to control expression values (vs. GAPDH) and the SEM (error bars). **, $p < .01$; *, $p < .05$; *t* test. Abbreviations: GFAP, glial fibrillary acidic protein; EdU, 5-ethynyl-2′-deoxyuridine; dSVZ, dorsal subventricular zone; lSVZ, lateral subventricular zone; LV, lateral ventricle; FOV, field of view.

Wnt-target gene induction in the lSVZ following infusion of AR-A014418 revealed no changes unlike in the dSVZ (Supporting Information Fig. S2). Together, these results identify that functional Wnt/β-catenin signaling is localized specifically to NSCs within the dSVZ microdomain and their neuronal and oligodendroglial progeny.

Wnt/β-Catenin Signaling Stimulates Proliferation in the Postnatal SVZ

The results presented above demonstrate that infusion of AR-A014418 stimulates Wnt/β-catenin signaling in the dSVZ and so we used this approach to examine the effects of β-catenin signaling on postnatal SVZ-NSCs, as in a previous study in the adult mouse SVZ [18]. Furthermore, we wished to clarify whether Wnt/β-catenin in the postnatal SVZ controls proliferation [18] or differentiation [19]. Pups aged P4 were infused with AR-A014418 or sterile vehicle as controls for 2 days and the SVZ analyzed at P6 by immunostaining for NSCs/cycling cells and rt-qPCR of NSC and SVZ cell markers (Fig. 3). As described previously [3], GFAP+ NSCs (type-B) in the postnatal SVZ were identified by their radial glia-like morphology, with cell bodies within the luminal wall of the ventricle and an apical primary process extending into the SVZ (Fig. 3A–3C). GFAP immunodetection was combined with EdU to further determine their cycling behavior as previous [9]. Mash1 and Dcx immunostaining were used in combination with EdU to identify transiently amplifying cells (type-C, Fig. 3D–3F) and type-A cells (Supporting Information Fig. S3A–S3C), respectively. Infusion of AR-A014418 significantly increased GFAP+ NSCs (both total and actively proliferating, i.e. EdU+) by a similar proportion in both dSVZ and lSVZ microdomains (Fig. 3A–3C; $p < .01$, *t* test). Similarly, the numbers of actively proliferating type-C cells were augmented by a similar proportion in either SVZ region (Fig. 3D–3F). Finally, Dcx+ neuroblast numbers (type-A cells, Supporting Information Fig. S3A–S3C; $p < .05$; *t* test) increased in both walls, although there were no significant changes in their proliferative behaviors. Overall, the extent of effects of AR-A014418 on proliferation was however higher in the dSVZ than lSVZ, as revealed by densitometry measurements of Proliferating Cell Nuclear Antigen positive (PCNA+) cells (Supporting Information Fig. S3D–S3F; $p < .05$, ANOVA followed by Bonferroni's post hoc tests). In addition, we used rt-qPCR of the dSVZ to examine expression of transcripts enriched in type-B, type-C, and type-A cells as well as ependymal and glial cells [30]. Markers for type-B and type-C cells i.e. Dlx4, ABCG2, Nestin, and PCNA were significantly increased in the dSVZ 2.5 hours after AR-A014418 infusion (Fig. 3G; $p < .05$, *t* test), whereas Dcx was not significantly altered at the mRNA level at this early time point, and neither were markers of other cells that reside in the SVZ (Fig. 3G). Taken together, these results support the evidence that postnatally, Wnt/β-catenin promotes neurogenesis through increased proliferation of both stem and progenitor cells in either SVZ microdomain.

Wnt/β-Catenin Signaling Regulates Neurogenesis and Oligodendrogenesis in the Postnatal dSVZ Microdomain

We examined the persistent role of Wnt/β-catenin in postnatal dSVZ-NSC specification using both gain- and loss-of-function approaches. Gain-of-function was induced genetically in $\beta\text{-catenin}^{exon3}$ mice, in which Cre-mediated recombination results in a constitutive stabilized form of β-catenin [24] (Fig. 4), or by AR-A014418 infusion in wild-type mice (Fig. 5). Electroporation of GFP plasmid or Cre:GFP plasmid was performed to target specifically defined microdomains of the SVZ, as previously reported [8]. All Cre:GFP transfected cells expressed the Cre recombinase as confirmed by immunostaining (Supporting Information Fig. S4). GFP-expressing electroporated cells were identified by immunostaining for lineage-specific markers: Tbr2 for glutamatergic NPs, Dlx2 for GABAergic NPs, and Olig2 for OPs [9, 13]. In targeting the specific microdomains of the SVZ, only NSCs in contact with the ventricular surface incorporate plasmids that are nonintegrating in the genome [8, 31]. The numbers of subsequent progeny expressing GFP 48 hour's post-transfection yield on average 446.2 transfected cells in five serial sections encompassing the entire rostral-caudal axis of the LV (Supporting Information Fig. S1). This approach allows a homogeneous sampling of sufficient numbers of fate-mapped NPs as described previously [9]. Following dorsal electroporation of $\beta\text{-catenin}^{exon3}$ mice (Fig. 4A–4D), many GFP+ cells could be seen expressing Tbr2 or Olig2 (Fig. 4A, 4C), whereas fewer expressed Dlx2 (Fig. 4A). In the dSVZ, β-catenin gain-of-function by Cre-recombination in $\beta\text{-catenin}^{exon3}$ mice resulted in a profound and significant increase in the numbers of Tbr2+/GFP+ NPs (Fig. 4A, 4B) and Olig2+/GFP+ OPs (Fig. 4C, 4D), together with a concomitant and a proportional decrease in Dlx2+/GFP+ cells (Fig. 4A, 4B). Notably, targeted genetic activation of Wnt/β-catenin in the lSVZ of the $\beta\text{-catenin}^{exon3}$ mouse did not induce Tbr2 or Olig2 expression in GFP+ cells (Fig. 4E–4H). Similar results were obtained following pharmacological stimulation of β-catenin. Infusion of AR-A014418 promoted the numbers of GFP+/Tbr2+ NPs (Fig. 5A–5C) and GFP+/Olig2+ OPs (Fig. 5D–5F) while decreasing the number of GFP+/Dlx2+ NPs. Furthermore, rt-qPCR of the microdissected dSVZ following AR-A014418 infusion demonstrated a specific increase in the dSVZ-NPs and OL lineage transcription factors and markers by more than 2-fold ($p < .01$, *t* test), whereas the lSVZ transcription factor Dlx2 was approximately halved (Fig. 5G). Interestingly, the early dSVZ marker Emx1 was unaffected, indicating Wnt/β-catenin signaling acts downstream of this transcription factor.

The genetic and AR-A014418 gain-of-function data showed that Wnt/β-catenin stimulates differentiation of dSVZ-NSCs along a glutamatergic NP and OP fate. This was examined further by genetic loss-of-function in $\beta\text{-catenin}^{lox/lox}$ and $\beta\text{-catenin}^{dm/lox}$ mice, the former to assess ablation of the entire β-catenin coding sequence [25], and the latter to assess exclusive ablation of canonical Wnt pathway activity, but retaining the cell adhesion function of β-catenin [26]. Targeted Cre-recombination in dSVZ-NSCs had equivalent effects in both transgenic mice, resulting in significant decreases in Tbr2+/GFP+ NPs and increases in Dlx2+/GFP+ NPs (Fig. 6A–6C; see graphs for *p* values). These gain- and loss-of-function findings demonstrate a novel functional role for the signaling form of β-catenin in dorsalization of the SVZ and indicate that it is necessary and sufficient for specification of NSCs toward the glutamatergic NP lineage. Interestingly, β-catenin loss-of-function did not alter the proportions of Olig2+/GFP+ OPs (Fig. 6D–6F), contrasting with the effects of β-catenin gain-of-function (Figs. 4C, 4D, 5D-F), and indicating that Wnt/β-catenin acts in concert with other signaling pathways to regulate oligodendrogliogenesis in the dSVZ.

Discussion

The function of Wnt/β-catenin signaling on the genesis of specific neuronal lineages from spatially segregated dorso-

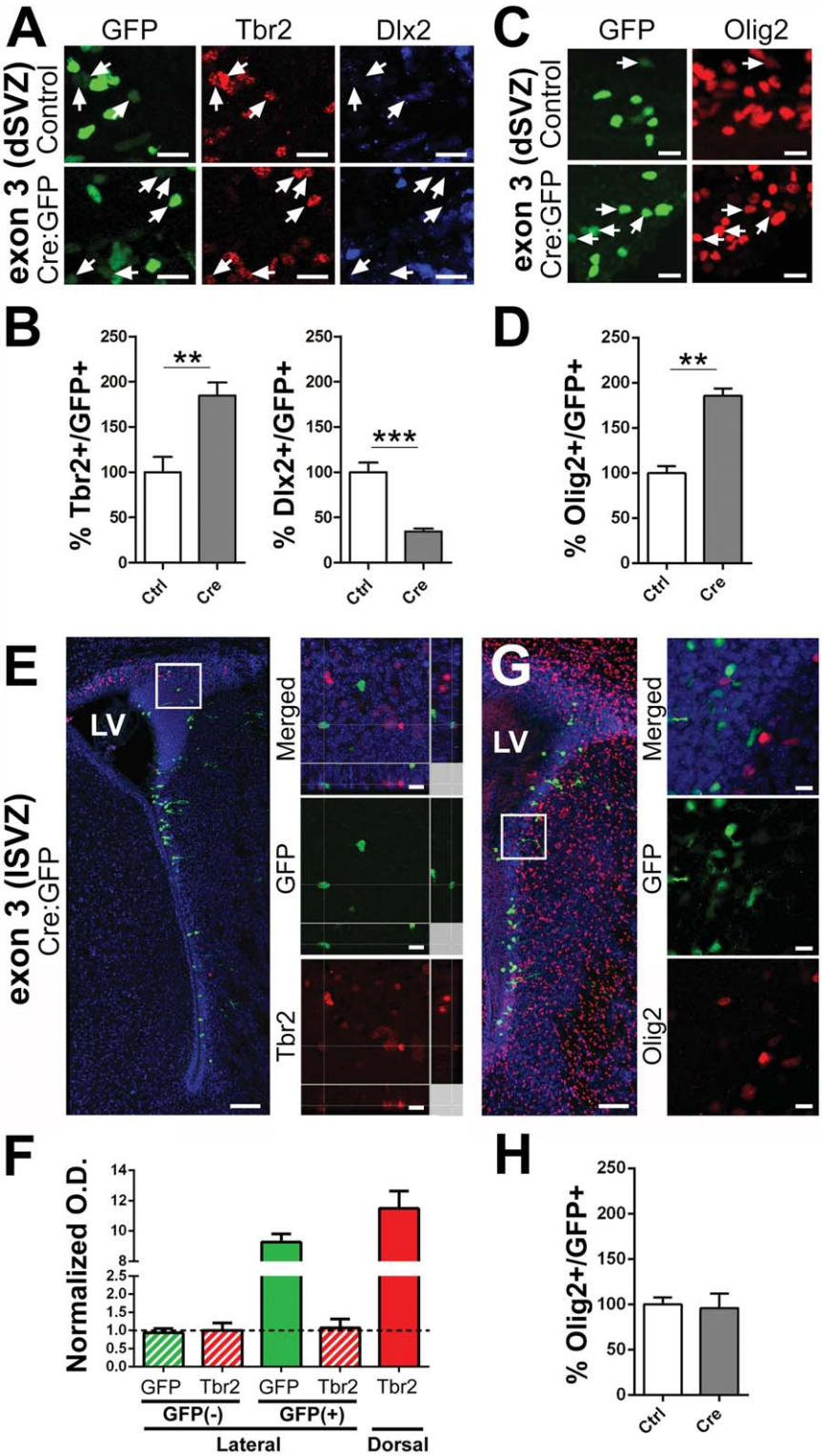

Figure 4. Genetic Wnt/β-catenin gain-of-function promotes glutamatergic neuronal precursors (NPs) and oligodendrocyte precursors (OPs) generation from NSCs located in the dSVZ. Pups were electroporated at P2 with a control pCAG-NLS-GFP plasmid or a pCAG-NLS-Cre:GFP to induce recombination into defined walls of the SVZ of β-catenin^{exon3} floxed animals. Animals were sacrificed at P6 for immunolabeling for lineage-specific markers. **(A, B):** The percentage of glutamatergic Tbr2+/GFP+ (arrows in A) *versus* GABAergic Dlx2+/GFP+ NPs was assessed following dorsal electroporation of a GFP plasmid (Control; top panels of A) or following Cre-mediated recombination (bottom panels of A) through the rostro-caudal axis of the LV and presented in B. **(C):** Similarly, the percentage of Olig2+/GFP+ OPs (arrows in C) was quantified following dorsal electroporation of a GFP plasmid (top panels of C) or following Cre-mediated recombination (bottom panels of C). (B, **D**): Quantification of Cre-mediated β-catenin^{exon3} stabilization resulted in an approximate doubling of the number of Tbr2+/GFP+ and a concomitant decrease of Dlx2+/GFP+ cells (B). A similar doubling of the number of Olig2+/GFP+ was observed (D). **(E):** Stabilization of β-catenin into the lateral wall failed to induce ectopic expression of Tbr2. Overview in (E) illustrates the exclusive location of electroporated cells to the lSVZ. The box indicates a region where NPs from the dSVZ and lSVZ migrate and mix together. Magnification of this region (right panels) showing absence of Tbr2 expression in lSVZ electroporated cells following stabilization of β-catenin. **(F):** Densitometry measurements of Tbr2 expression within GFP+ transfected cells *versus* neighboring GFP− cells confirmed absence of Tbr2 expression while Tbr2+ cells in the dSVZ showed high O.D. values for this marker. **(G):** Similarly, stabilization of β-catenin into the lateral wall failed to induce ectopic expression of Olig2. Only rare Olig2+/GFP+ cells were observed following electroporation of the lSVZ and their number did not change following β-catenin stabilization **(H)**. Scale bars = 10 μm in (A) and (C); 250 μm (overviews) and 10 μm (insets) in (E) and (G). Quantifications in (B), (D), and (H) are normalized to corresponding averaged control values and the SEM (error bars); $n > 4$ animals throughout. ***, $p < .001$; **, $p < .01$; *t* test. Abbreviations: dSVZ, dorsal subventricular zone; GFP, green fluorescent protein; lSVZ, lateral SVZ; LV, lateral ventricle; Cre, Cre recombinase; Ctrl, Control; O. D., Optical Densitometry.

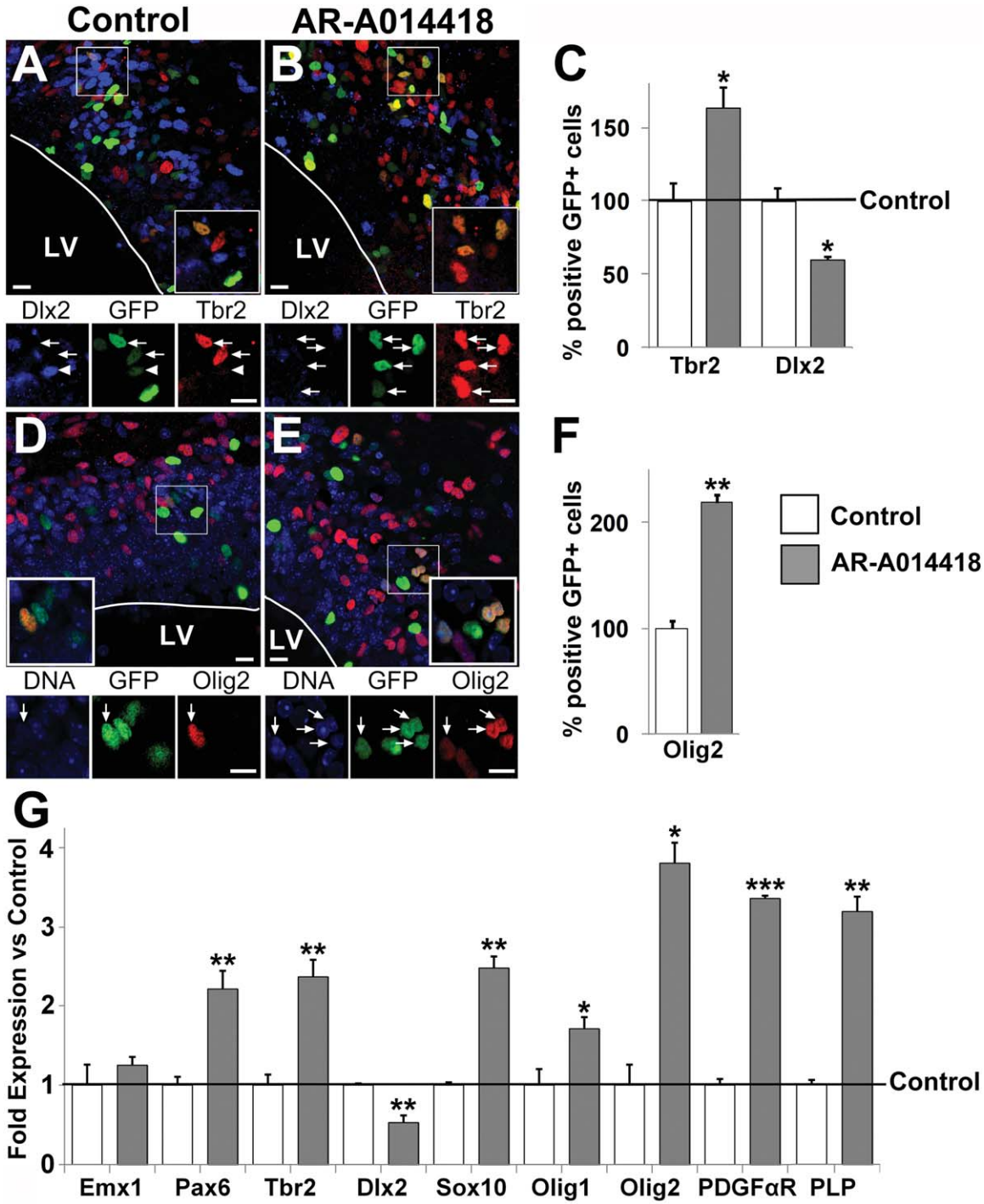

Figure 5. Pharmacological Wnt/β-catenin gain-of-function promotes glutamatergic neuronal precursors and oligodendrocyte precursors generation from NSCs located in the dSVZ. Pups were electroporated at P3 in the dSVZ with pCAG-NLS-GFP plasmid and treated with AR-A014418 or vehicle (saline/DMSO) for the following 2 days. All animals were sacrificed at P6 for immunolabeling of defined lineages. **(A, B):** Confocal images (maximal intensity projection of a 10 μm stack) illustrating that GFP+ cells expressed Tbr2 (arrows) or Dlx2 (arrowheads) in controls (A) and following AR-A014418 treatment (B). Single plane images of the boxed areas are shown at higher magnifications as merged images (insets) and single channel images (captions). **(C):** Quantifications show an increase of the number of Tbr2+/GFP+ and a concomitant decrease of the number of Dlx2+/GFP+ following AR-A014418 treatment. **(D, E):** Olig2+/GFP+ OPs were few in controls (D, arrows) and these increased following AR-A014418 treatment (E), as quantified in **(F)**. Quantifications in (C) and (F) are normalized to corresponding averaged control values. Scale bars = 10 μm. **(G):** AR-A04418 or saline/DMSO was infused intraventricularly and the dSVZ microdissected for subsequent real-time quantitative polymerase chain reaction determination of selected transcription factor and lineage marker transcripts. Changes in transcripts expression levels in (G) are normalized to GAPDH. Error bars represent the SEM ($n \geq 4$ animals in C and F; $n > 3$; three animals pooled per n number in G). ***, $p < .001$; **, $p < .01$; *, $p < .05$; t test. Abbreviations: GFP, green fluorescent protein; LV, lateral ventricle; PLP, Myelin Proteolipid Protein; PDGFαR, platelet-derived growth factor-α receptor.

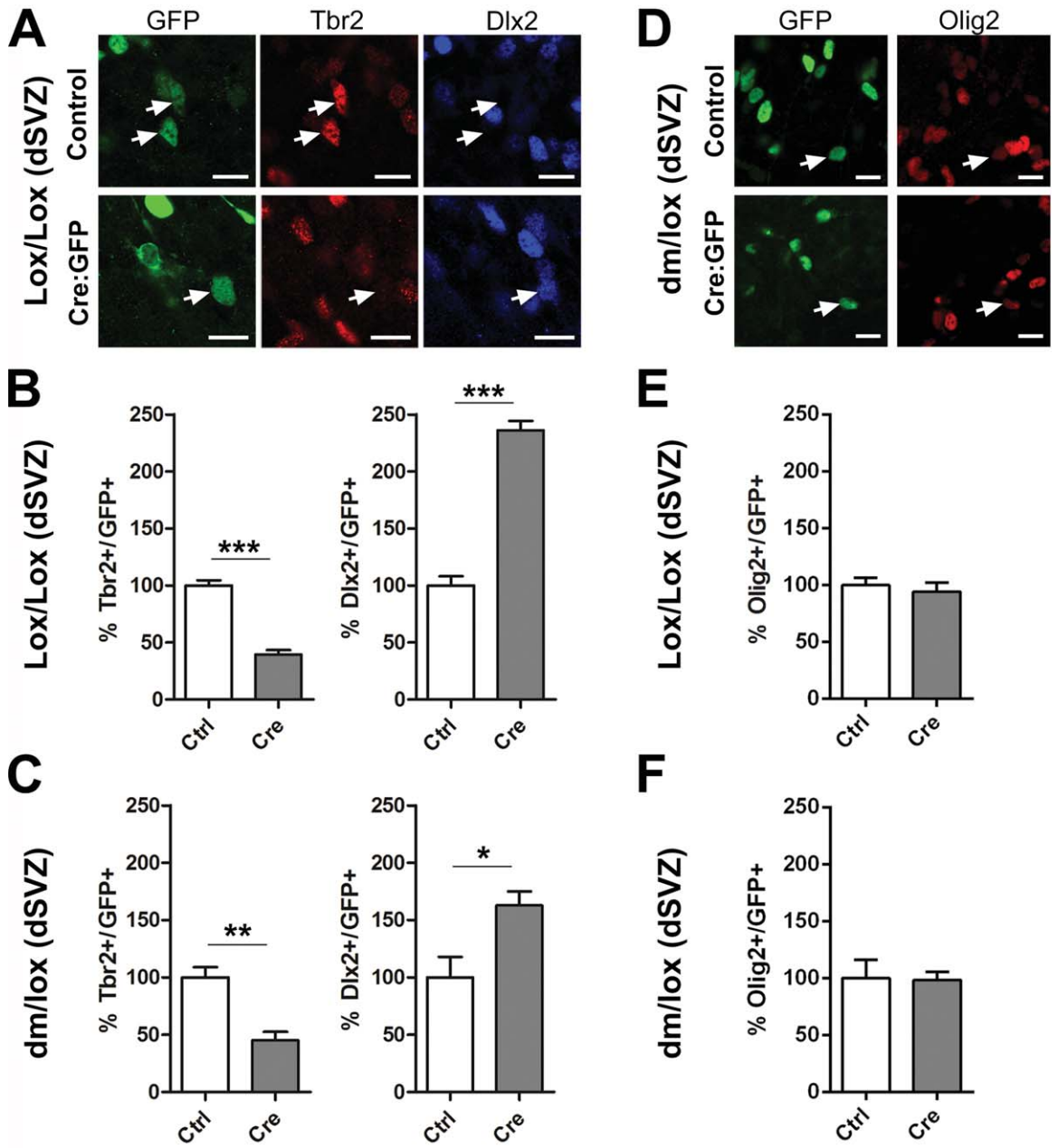

Figure 6. Genetic Wnt/β-catenin loss-of-function affects neuronal specification but not oligodendrogenesis in the dSVZ. Pups aged P2 were electroporated with a control pCAG-NLS-GFP plasmid or a pCAG-NLS-Cre:GFP and sacrificed at P6 for immunolabeling of specific lineages. Transgenic lines were either β-catenin floxed animals (β-catenin$^{lox/lox}$) for ablation of the entire coding sequence or signaling mutant animals (β-catenin$^{dm/lox}$) for deletion of β-catenin transcription factor binding domains. **(A–C):** The percentage of glutamatergic Tbr2+/GFP+ *versus* GABAergic Dlx2+/GFP+ NPs was assessed following dorsal electroporation of a GFP plasmid (top panels of A) or following Cre-mediated recombination (bottom panels of A). Cre-mediated recombination resulted in a decrease in the percentage of Tbr2+/GFP+ cells and a concomittant increase in the percentage of Dlx2+/GFP+ cells. **(D–F):** Similarly, the percentage of Olig2+/GFP+ OPs was quantified following dorsal electroporation of a GFP plasmid (top panels of D) or following Cre-mediated recombination (bottom panels of D). Quantifications for Olig2+/GFP+ in β-catenin$^{lox/lox}$ (E) and β-catenin$^{dm/lox}$ (F) showed no change in the percentage of Olig2+/GFP+. Scale bars = 10 μm. Arrows indicate GFP+/Tbr2+/Dlx2- cells in (A) and GFP+/Olig2+ cells in (D). All quantifications are normalized to corresponding averaged control values. Error bars represent the SEM of $n > 4$ animals throughout; ***, $p < .001$; **, $p < .01$; *, $p < .05$; *t* test. Abbreviations: dSVZ, dorsal subventricular zone; GFP, green fluorescent protein; Cre, Cre-recombinase; Ctrl, Control.

ventral sources is recognized during early embryonic forebrain development. However, relatively little was known about the effect of Wnt/β-catenin signaling on postnatal neurogenesis. In this study, we show by rt-qPCR that Wnt/β-catenin signaling is restricted to the dorsal microdomain of the postnatal SVZ, and analysis of the Bat-Gal reporter mouse [23] demonstrated that functional Wnt/β-catenin signaling is localized to dorsally located NSCs and actively

proliferative transient amplifying cells that generate OPs and glutamatergic NPs. Furthermore, genetic and pharmacological *in vivo* gain- and loss-of-function approaches demonstrate that β-catenin signaling regulates both proliferation and NP lineage choice in the dSVZ. The results of this study identify the dSVZ of the postnatal brain as a previously unrecognized niche for Wnt/β-catenin signaling, which specifically regulates the generation of glutamatergic NPs and OPs from dSVZ-NSCs.

Our expression profiling of the microdissected SVZ shows that spatially restricted populations of NSCs persist in the SVZ after birth and express lineage-specific transcription factors that determine their neurogenic fate. These results together with previous fate mapping studies demonstrate that Olig2+ OPs and Tbr2+ olfactory glutamatergic NPs derive from the dSVZ microdomain, whereas Dlx2+ GABAergic NPs derive from both the dSVZ and lSVZ [7, 12–15]. The heterogeneity of SVZ-NSCs was originally thought to be intrinsically coded [7], but our expression profiling in microdissected SVZ identifies canonical Wnts as the key dorsalizing factor in the postnatal SVZ, opposing ventrally localized Shh activity to determine dorso-ventral NSC fate [16, 17, 32]. Functional β-catenin expression was examined by immunodetection of βGal in Wnt-signaling reporter mice [23]. Wnt/β-catenin activity was highest in GFAP+ NSCs and actively proliferating transiently amplifying (type-C) cells of the dSVZ, supporting observations in the embryonic and adult brain [18, 33]. In addition, using infusion of the GSK3β inhibitor AR-A014418 to inhibit phosphorylation of β-catenin and stimulate its nuclear translocation, we demonstrate that endogenous β-catenin is highly localized to the dSVZ, and results in activation of canonical Wnt/β-catenin targets Tcf and Lef1 as well as Fzd1 and Axin2. Activation of β-catenin activity stimulated proliferation most dramatically in the dSVZ microdomain, consistent with other studies using *in vitro* and *in vivo* approaches [18, 22]. A new finding is that the highest functional Wnt/β-catenin activity defines the dSVZ-NSCs and their progeny, Tbr2+ NPs and Olig2+ OPs. Furthermore, AR-A014418 did not affect expression of Gli1, a downstream target of Shh signaling in dSVZ-NSCs [32], which maintains ventralization of the postnatal SVZ [34], providing further evidence that Wnt/β-catenin signaling exerts a direct dorsalizing effect on the postnatal SVZ.

We could confirm an augmentation of NSCs and progenitor cell number and proliferation in the lSVZ following AR-A014418 infusion. A similar increase has been previously described at E13.5 following ablation of GSK3β in NSCs [35] as well as in the adult mouse using other GSK3β inhibitors [18]. In this study, these effects are unlikely to involve activation of the canonical Wnt pathway as no induction of downstream Wnt/β-catenin-target genes was detected in the lSVZ following AR-A014418 infusion. The effects of GSK3β inhibition in promoting neurogenesis from the lSVZ involve other signaling pathways. In addition to the increase proliferation which was more pronounced in the dSVZ, our β-catenin gain- and loss-of-function studies underline that Wnt/β-catenin regulates fate specification of dSVZ-NSCs. Analysis of NSC progeny following genetic or pharmacological stimulation of β-catenin demonstrated more Tbr2+ NPs at the expense of Dlx2+ NPs. Consistently, targeted genetic ablation of β-catenin activity in dSVZ-NSC had the opposite effect, resulting in a marked decrease in Tbr2+ NPs and a proportional increase in Dlx2+ NPs. It is noteworthy that targeted genetic stimulation of β-catenin activity in NSCs of the lSVZ failed to induce Tbr2 expression. This nonpermissiveness of lSVZ-NSC appears to be a postnatal acquisition, since embryonic respecification of ventral NSCs can be achieved by expression of constitutively active β-catenin, resulting in partial expression of dorsally restricted markers in the ventral forebrain (most notably Ngn2) and a decrease in expression of ventral-restricted markers [17].

An important finding is that Wnt/β-catenin is a profound positive regulator of oligodendrogliogenesis from dSVZ-NSCs. Notably, our studies indicate OL lineage cells are largely derived from the dSVZ microdomain, together with glutamatergic NPs. Moreover, we failed to induce ectopic generation of OPs in the lSVZ following genetic or pharmacological stimulation of β-catenin activity. This contrasts with the effects of FGF2, which we have shown to promote ectopic generation of OPs from the lSVZ [15]. In confirmation of our fate-mapping results, transcripts for more differentiated OL lineage cells, PDGFαR and PLP, were markedly increased by AR-A014418, consistent with our previous study showing that AR-A014418 promotes differentiation as well as proliferation of OL lineage cells [21]. Our findings are in line with a recent parallel study showing that *in vivo* activation of canonical Wnt signaling increased the generation of Olig2+ and PDGFαR+ OPs in the adult SVZ [22], but do not support the conclusion that Wnt/β-catenin is selective for OL lineage cells. Indeed, as discussed above, our studies clearly demonstrates that Wnt/β-catenin also promotes neurogenesis and regulates NP fate along the glutamatergic *versus* the GABAergic lineage. Interestingly, oligodendrogliogenesis was promoted by stimulation of β-catenin signaling, but was unaffected by genetic inhibition of β-catenin, in contrast to neurogenesis, which was affected by both β-catenin gain- and loss-of-function. These results suggest Wnt/β-catenin is necessary and sufficient for specification of NSCs along the glutamatergic NP lineage, but acts in concert with other factors to regulate oligodendrogliogenesis [15, 21].

Conclusion

In conclusion, this study highlights a novel role for Wnt/β-catenin signaling in promoting glutamatergic neurogenesis and oligodendrogliogenesis from the dorsal microdomain of the postnatal SVZ.

Acknowledgments

K.A., B.F., and A.H.C. are supported by a National Research Project Grant (NRP63; 406340_128291) and from a research Grant (31003A_127082) from the Swiss National Fund. K.A. and A.B. are funded in part by the Multiple Sclerosis Society of the UK. K.A. also received support from the Forschungskredit (K-41211-01-01) of the University of Zurich. A.H.C. is also supported by a grant from the Mexican Government (CONACYT). This work was performed within the program "Investissements d'Avenir" (ANR-11-IDEX-0007) operated by the French National Research Agency (ANR).

Author Contributions

K.A. and B.F.: collection and assembly of data, data analysis interpretation, and manuscript writing; A.H.C., K.D., C.C., and M.Z.: provision of study material, collection, and assembly of data; L.S.: provision of study material and final approval of manuscript; A.B. and O.R.: conception and design, data analysis interpretation, manuscript writing, and final approval of manuscript. K.A. and B.F. contributed equally to this article.

Disclosure of Potential Conflicts of Interest

The authors indicate no potential conflicts of interest.

References

1 Lois C, Alvarez-Buylla A. Long-distance neuronal migration in the adult mammalian brain. Science 1994;264:1145–1148.

2 Menn B, Garcia-Verdugo JM, Yaschine C et al. Origin of oligodendrocytes in the subventricular zone of the adult brain. J Neurosci 2006;26:7907–7918.

3 Doetsch F, Caille I, Lim DA et al. Subventricular zone astrocytes are neural stem cells in the adult mammalian brain. Cell 1999;97:703–716.

4 Doetsch F, Garcia-Verdugo JM, Alvarez-Buylla A. Cellular composition and three-dimensional organization of the subventricular germinal zone in the adult mammalian brain. J Neurosci 1997;17:5046–5061.

5 Lledo PM, Merkle FT, Alvarez-Buylla A. Origin and function of olfactory bulb interneuron diversity. Trends Neurosci 2008;31:392–400.

6 Kessaris N, Fogarty M, Iannarelli P et al. Competing waves of oligodendrocytes in the forebrain and postnatal elimination of an embryonic lineage. Nat Neurosci 2006;9:173–179.

7 Merkle FT, Mirzadeh Z, Alvarez-Buylla A. Mosaic organization of neural stem cells in the adult brain. Science 2007;317:381–384.

8 Fernandez ME, Croce S, Boutin C et al. Targeted electroporation of defined lateral ventricular walls: A novel and rapid method to study fate specification during postnatal forebrain neurogenesis. Neural Dev 2011;6:13.

9 Azim K, Fiorelli R, Zweifel S et al. 3-dimensional examination of the adult mouse subventricular zone reveals lineage-specific microdomains. PLoS ONE 2012;7:e49087.

10 Kelsch W, Mosley CP, Lin CW et al. Distinct mammalian precursors are committed to generate neurons with defined dendritic projection patterns. PLoS Biol 2007;5:e300.

11 Young KM, Fogarty M, Kessaris N et al. Subventricular zone stem cells are heterogeneous with respect to their embryonic origins and neurogenic fates in the adult olfactory bulb. J Neurosci 2007;27:8286–8296.

12 Brill MS, Ninkovic J, Winpenny E et al. Adult generation of glutamatergic olfactory bulb interneurons. Nat Neurosci 2009;12:1524–1533.

13 Winpenny E, Lebel-Potter M, Fernandez ME et al. Sequential generation of olfactory bulb glutamatergic neurons by Neurog2-expressing precursor cells. Neural Dev 2011;6:12.

14 Kohwi M, Petryniak MA, Long JE et al. A subpopulation of olfactory bulb GABAergic interneurons is derived from Emx1- and Dlx5/6-expressing progenitors. J Neurosci 2007;27:6878–6891.

15 Azim K, Raineteau O, Butt AM. Intraventricular injection of FGF-2 promotes generation of oligodendrocyte-lineage cells in the postnatal and adult forebrain. Glia 2012;60:1977–1990.

16 Ihrie RA, Shah JK, Harwell CC et al. Persistent sonic hedgehog signaling in adult brain determines neural stem cell positional identity. Neuron 2011;71:250–262.

17 Backman M, Machon O, Mygland L et al. Effects of canonical Wnt signaling on dorso-ventral specification of the mouse telencephalon. Dev Biol 2005;279:155–168.

18 Adachi K, Mirzadeh Z, Sakaguchi M et al. Beta-catenin signaling promotes proliferation of progenitor cells in the adult mouse subventricular zone. Stem Cells 2007;25:2827–2836.

19 Marinaro C, Pannese M, Weinandy F et al. Wnt signaling has opposing roles in the developing and the adult brain that are modulated by Hipk1. Cereb Cortex 2011;22:2415–2427.

20 Fancy SP, Baranzini SE, Zhao C et al. Dysregulation of the Wnt pathway inhibits timely myelination and remyelination in the mammalian CNS. Genes Dev 2009;23:1571–1585.

21 Azim K, Butt AM. GSK3beta negatively regulates oligodendrocyte differentiation and myelination in vivo. Glia 2011;59:540–553.

22 Ortega F, Gascon S, Masserdotti G et al. Oligodendrogliogenic and neurogenic adult subependymal zone neural stem cells constitute distinct lineages and exhibit differential responsiveness to Wnt signalling. Nat Cell Biol 2013;15:602–613.

23 Maretto S, Cordenonsi M, Dupont S et al. Mapping Wnt/beta-catenin signaling during mouse development and in colorectal tumors. Proc Natl Acad Sci USA 2003;100:3299–3304.

24 Harada N, Tamai Y, Ishikawa T et al. Intestinal polyposis in mice with a dominant stable mutation of the beta-catenin gene. EMBO J 1999;18:5931–5942.

25 Brault V, Moore R, Kutsch S et al. Inactivation of the beta-catenin gene by Wnt1-Cre-mediated deletion results in dramatic brain malformation and failure of craniofacial development. Development 2001;128:1253–1264.

26 Valenta T, Gay M, Steiner S et al. Probing transcription-specific outputs of beta-catenin in vivo. Genes Dev 2011;25:2631–2643.

27 Marques F, Sousa JC, Coppola G et al. Transcriptome signature of the adult mouse choroid plexus. Fluids Barriers CNS 2011;8:10.

28 Bowyer JF, Thomas M, Patterson TA et al. A visual description of the dissection of the cerebral surface vasculature and associated meninges and the choroid plexus from rat brain. J Vis Exp 2012:69:e4285.

29 Johansson PA, Irmler M, Acampora D et al. The transcription factor Otx2 regulates choroid plexus development and function. Development 2013:140:1055–1066.

30 Beckervordersandforth R, Tripathi P, Ninkovic J et al. In vivo fate mapping and expression analysis reveals molecular hallmarks of prospectively isolated adult neural stem cells. Cell Stem Cell 2010:7:744–758.

31 Boutin C, Hardt O, de Chevigny A et al. NeuroD1 induces terminal neuronal differentiation in olfactory neurogenesis. Proc Natl Acad Sci USA 2010:107:1201–1206.

32 Palma V, Lim DA, Dahmane N et al. Sonic hedgehog controls stem cell behavior in the postnatal and adult brain. Development 2005:132:335–344.

33 Backman M, Machon O, Mygland L et al. Effects of canonical Wnt signaling on dorso-ventral specification of the mouse telencephalon. Dev Biol 2005:279:155–168.

34 Vokes SA, Ji H, McCuine S et al. Genomic characterization of Gli-activator targets in sonic hedgehog-mediated neural patterning. Development 2007:134:1977–1989.

35 Kim WY, Wang X, Wu Y et al. GSK-3 is a master regulator of neural progenitor homeostasis. Nat Neurosci 2009:12:1390–1397.

See www.StemCells.com for supporting information available online.